IEEE Access
Multidisciplinary | Rapid Review | Open Access Journal

Received December 2, 2020, accepted December 13, 2020, date of publication December 16, 2020,
date of current version December 31, 2020.

Digital Object Identifier 10.1109/ACCESS.2020.3045163

Dual Adaptive Model Predictive Controller Application to Vertical Roller Mill Process Used in the Cement Industry

B. VIJAYABHASKAR AND S. JAYALALITHA
School of Electrical and Electronics Engineering, SASTRA Deemed University, Thanjavur 613401, India
Corresponding author: B. Vijayabhaskar (vijayabhaskar@eie.sastra.edu)

ABSTRACT Diversified operating conditions, input-output constraints, and parametric variations in the Vertical Roller Mill (VRM) make it to have complicated dynamics and closed-loop instability. Existing traditional controllers are not superlative and may lead to an uneven plant shutdown. Model predictive controller with adaptive models can track these parametric variations and ensure the plant's smooth running, which has been addressed in this paper. Data from the real-time VRM is acquired, and correlation analysis is carried out, which illustrates the use of outlet temperature and differential pressure as the output variables with tensile pressure and booster fan speed as the input variables. The base model for VRM is identified using the selected variables by data-driven system identification methods. The fourth-order state-space model was found to be optimal in capturing the dynamic behavior of VRM. Dual Adaptive Model Predictive Controller (DAMPC) is designed to handle each output variable individually. The use of DAMPC minimizes the complexity involved in the on-line parametric estimation for higher-order models by distributing the control authority to different controllers. The performance of the proposed DAMPC is compared with the existing Proportional Integral (PI) controller and Model Predictive Controller (MPC). Simulation experiments for reference tracking and rejection of slowly varying internal disturbances by considering parametric variations are carried out. Results illustrate DAMPC provides lesser overshoot and faster settling time amidst parametric variations.

INDEX TERMS Adaptive model predictive control, extended least square, recursive polynomial estimator, system identification, vertical roller mill.

ABBREVIATIONS

AIC:	Akaike Information Criteria
AMPC:	Adaptive Model Predictive Controller
ARMAX:	Autoregressive Moving Average with Extra Input
ARX:	Autoregressive with Extra Input
BFS:	Booster Fan Speed
BIC:	Bayesian Information Criterion
BJ:	Box-Jenkins
CFS:	Classifier Fan Speed
CQ:	Cement Quality
DAMPC:	Dual Adaptive Model Predictive Controller
DP:	Differential Pressure
ELS:	Extended Least Square
FOPID:	Fractional Order Proportional Integral Derivative
FPE:	Final Prediction Error
GBBDV:	Gear Box Body Vibrations
GBBV:	Gear Box Base Vibrations
GBSV:	Gear Box Shaft Vibrations
IAE:	Integral Absolute Error
ISE:	Integral Square Error
ITAE:	Integral Time Absolute Error
ITSE:	Integral Time Square Error
MBT:	Mill Bed Thickness
MDL:	Mill Drive Load
MFS:	Mill Fan Speed
MIF:	Mill Inlet Feed
MIMO:	Multi-Input Multi-Output
MISO:	Multi-Input Single-Output
MO:	Mill Outlet

The associate editor coordinating the review of this manuscript and approving it for publication was Mauro Gaggero.

MPC:	Model Predictive Controller
MR:	Mill Reject
MSE:	Mean Square Error
NLARX:	Nonlinear Autoregressive with Extra Input
NLHW:	Nonlinear Hammerstein-Wiener
OE:	Output Error
OPC:	Ordinary Portland Cement
OT:	Outlet Temperature
PD:	Process with Delay
PI:	Proportional Integral
PID:	Proportional Integral Derivative
PPC:	Pozzadona Portland Cement
RDP:	Recirculating Damper Position
RGA:	Relative Gain Array
SPC:	Specific Power Consumption
SS:	State-Space
TF:	Transfer Function
TMPC:	Total Mill Power Consumption
TP:	Tensile Pressure
VRM:	Vertical Roller Mill
WSPS:	Water Spray Pump Speed

I. INTRODUCTION

The sustainability of cement manufacturing has been struggling with high energy consumption and the gap between supply and demand. The electrical energy consumption for various phases in cement production is shown in Fig. 1. The grinding process of coal, raw material, and cement consumes 40%-70% of cement mill power consumption. Typically, the power consumption to produce ton cement is between 60 kWh-120 kWh. In the past, the application of VRMs, Horomills, and High-Pressure Grinding Rolls (HPGR) had substantiated and reduced the mill's power consumption. Some investigations observed that VRM installation in grinding saves 30% of cement mill energy with ease of control and reduces the mill start-up/shut down durations [1]–[5]. The VRM system for coal, cement, and raw material grinding is more successful due to low power consumption, simple circuit design, and flexible designs. An auxiliary facility for various operating parameters, one machine for crushing, grinding, drying, and separating makes VRM more reliable with a low noise level [6], [7]. Fig. 2 shows the VRM for cement grinding near Ariyalur, Tamilnadu, India, along with rollers and grinding table set-up.

A. THE GRINDING PROCESS IN VRM

The VRM consists of three or four stationary grinding rollers and the same number of supporting rollers (small in size depending on the different designs and manufacturers), and a whirling grinding table. Suitable pressure causes the material to strain in between the grinding table and rollers. A hydro-pneumatic tension system is used to supply the required pressure forces. The strained material is transported to a fixed nozzle ring owing to the revolution of the grinding table. The nozzle ring delivers the dried material to the classifier using the gas flow. The separator segregates material into fines and tailings; with the gas flow, fines leave the separator, and tailings fall back to the grinding zone [8], [9].

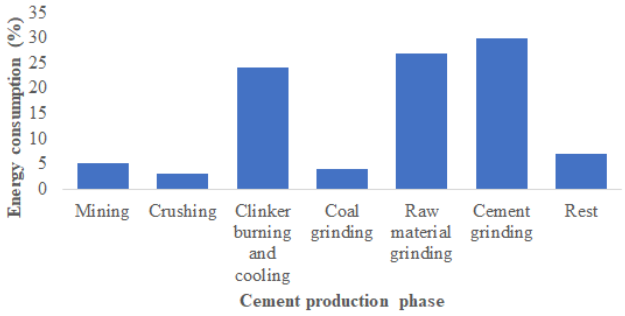

FIGURE 1. Electrical energy consumption for various phases in the cement industry.

B. PARAMETERS AFFECTING THE VRM PROCESS

The cement grinding performance is influenced by the grinding mill's design, process control, and air separator construction. Many design organizations developed various grinding machines to reduce the mill electric power consumption by optimally designing the clinker/cement grinding process within the industry's requirement. In VRMs, OT, DP, GBSV, MBT, CQ, etc., are controlled by manipulating the variables like MIF, CFS, WSPS, BFS, TP, MFS, etc. The monitoring and control of key process variables in the VRM play a significant role in the start-up and stabilization of the mill. The affect of different manipulated variables on the VRM process are described in Table 1.

Maintenance of these manipulated variables at desired values is critical in the cement eminence; otherwise, these variables influence the fineness with a high amount of dust and packing hasty setting. VRMs have the dynamics altering in 2-4 minutes; the rapid change in dynamics requires faster consideration of the process situations and enchanting perfect action in time. In some cement industries, nozzle ring and damping rings are adjusted to increase the cement's fineness. In most of the cement plants, proper control of VRM provides good fineness with reduced power consumption. Hence, a suitable control law is essential to bring these values desired during start-up and maintain the same while the plant is running.

C. PRESENT STATUS OF VRM PROCESS CONTROL

The efficient process control of VRM with the manipulated variables, applied pressure, airflow, and rotor speed of the classifier is discussed in some research articles. Some researchers constructed a mathematical model using the intelligent finite element analysis for VRM using vibration characteristics and concluded that these simplified models are not satisfactory for practical applications [1], [6], [8], [9]. Most of the research is focused on vibration analysis and control by manipulating the inlet feed. The parameters are considered by neglecting the interaction between the variables that causes

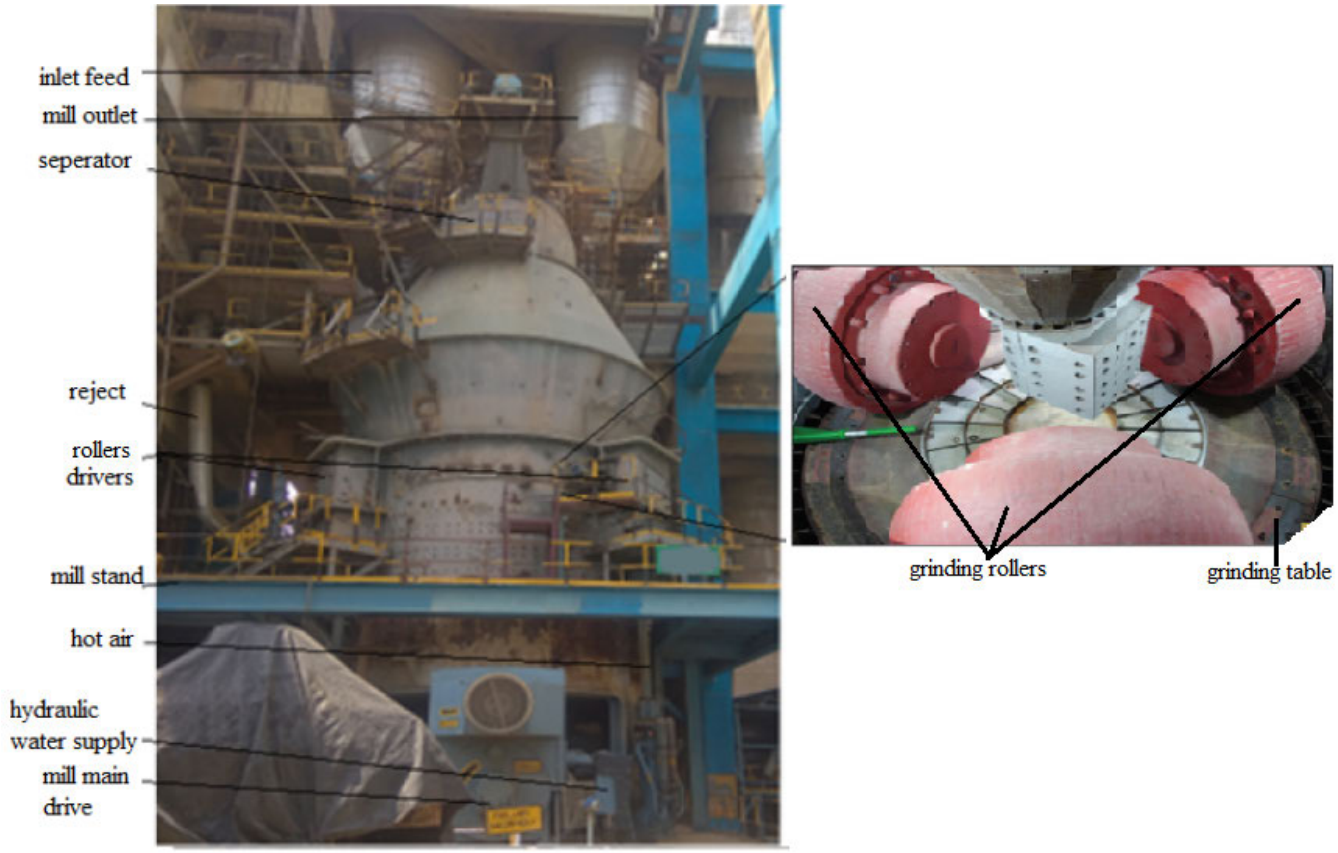

FIGURE 2. VRM process station installed for cement in Southern India with grinding table and rollers set-up.

TABLE 1. Different manipulated variables affect on the VRM process used in cement grinding [1], [7], [10]–[13].

		Output variables						
	Process variables	DP	TMPC	MR	GBSV	MBT	OT	CQ
Manipulated variables	MIF (+1)	-1	+1	+1	-1	+1	-1	-1
	BFS (+1)	-1	-1	0	0	0	+1	-1
	WSPS (+1)	+1	+1	-1	+1	-1	-1	+1
	CFS (+1)	+1	-1	+1	0	0	-1	-1
	MFS (+1)	0	+1	-1	0	0	0	0
	TP (+1)	+1	-1	0	+1	+1	-1	+1

* '+1' indicate increase in value, '-1' indicate decrease in value, and '0' indicate no change in value

practical difficulties in real-time applications. An expert system was constructed to deal with the vibrations, but the lack of prior knowledge about the variables' characteristic behavior limits its usage [14]. Some investigations using intelligent control divided the VRM process into many single loops like pressure, temperature, vibration, etc., and applied individual control algorithms. These control mechanisms produced satisfactory results only when all the process inputs are readily available within the constraints if any variable out of range causes the plant's uneven shutdown [7], [12], [15].

Most of the VRMs used in cement plants are still using either manual control by monitoring the process variables continuously or by adapting PID control or Fuzzy intelligent or Programmable Logic Controllers (PLC) or Neuro-fuzzy expert systems in individual loops [12], [16]. Many studies explained the equipment structure, process control loop selections, and process flow of VRM local loops. However, the complexity of the distribution and coupling of different loops reduces the overall optimization effect. The VRM process flow diagram used for cement grinding is shown in Fig. 3. Classical PID control methods are extensively used for the control of SISO feedback loops. PID controllers are inadequate for highly nonlinear plants, and tuning is not an easy task while handling the constraints. Therefore, the traditional control methods for nonlinear systems are infeasible [12]–[14]. Some investigations discussed the application of intelligent controllers, feedback, and feed-forward controllers by considering the disturbances and uncertainty to the plant. With little knowledge of the process, these methods provide adequate improvement in comparison with

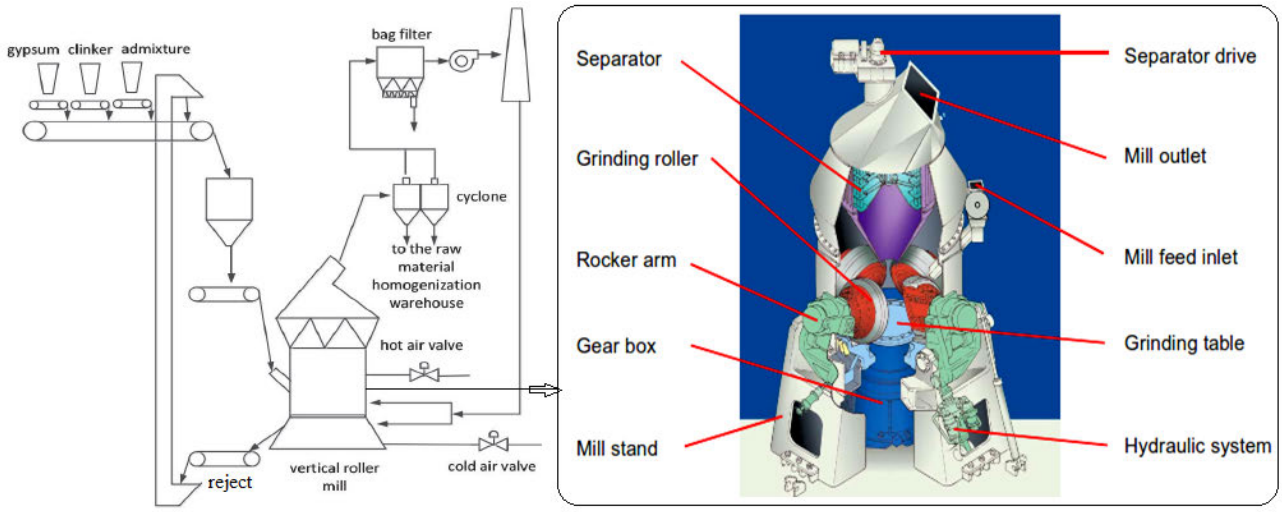

FIGURE 3. Cement VRM process flow along with an internal schematic diagram [12], [13].

traditional control methods. Still, these methods may not guarantee the stability of the system under parametric variations [17]. Some studies explored the grinding circuit control using advanced model predictive control to increase the throughput and fineness. The adaption of the modern control technique in industrial plants is expanding growth. The advancements in model-based control methods are preferred over the classical approaches due to their flexibility to operate for large operating ranges without re-tuning and the handling capacity of multi-variable systems. With the handling capability of state constraints and addressing the control law, MPC algorithms are more prevalent. Automatic control law adaption is limited to VRM due to the absence or lack of process variable measurements while controlling the plant [15], [18]. Some studies outlined overall grinding process optimization with on-line decision approaches using the cement plant [19]. With the support of operator assistance, these methods are not feasible for a complete mill. The multi-variable interacting nature, complex dynamics, nonlinear kinetics, and slowly varying feed characteristics make it challenging to implement a control strategy relying only on operator experience [20]–[22]. Different control methods used in VRM process are summarized in Table 2. Hence, to control the VRM more effectively, to produce accurate responses, and to improve time response characteristics, an AMPC based controller is proposed in this research work.

Data-based modeling and investigation of DAMPC for industrial VRM process with on-line parameter estimation are considered the novelty of the proposed work, which has not been attempted in the literature. The contribution of this paper can be summarized as follows:

1. The real-time working plant data is collected by visiting the cement plant. As per the grinding machine control engineer's suggestion, the data is preprocessed and then using different linear and nonlinear system identification methods, the satisfactory VRM model is identified.

2. In the cement manufacturing process, the same grinding machine is used to produce different cement types by changing the plant's inputs; hence, process parameters also change. We applied an on-line parameter estimation technique along with DAMPC to handle these parametric variations.

3. The proposed control method produces better reference tracking and transient response than the existing traditional control methods.

The rest of the paper is organized as follows: In Section II, the mathematical modeling of the VRM process is identified. Various process control methods for VRM are described in Section III. The performance of the proposed controller is verified through the simulation results and detailed in Section IV. Finally, the paper is concluded with the conclusion in Section V.

II. MATHEMATICAL MODELING OF VRM

The efficient process control of the plant depends on the availability of accurately predicted plant models. The first principle methods are not appropriate for the VRM process as the relations between the variables are not known. The VRM process exhibits highly nonlinear, unknown delay times, and more intricate dynamics; hence different block box modeling methods are used for model identification [28].

A. DATA COLLECTION AND PREPROCESSING

The cement is categorized as OPC (OPC-43, OPC-53, etc.) and PPC, depending on the clinker quality and different compositions used. The real-time plant data is collected from the cement plant near Ariyalur, India, to produce PPC cement. The compositions used in PPC are clinker 48%, wet fly ash, additive 16% (is called mega-mix), gypsum 2%, dry fly

TABLE 2. Comparison of various VRM process control methods.

Control method	Input variables	Output variables	Methodology used	Merits	Demerits
Cascaded control [11]	MIF, CFS	MO, CQ	individual PID controllers are used	good reference tracking	parametric variations not considered
FOPID [12]	BFS	OT	ITAE and ISE based	the range of adjustable parameters is more	overshoots present, more complex for MIMO systems
Intelligent control (Self-tuning PID) [23]	BFS, MIF	DP, OT	based on separate control loop for each variable	guaranteed stability and reliability	parametric changes and disturbances are not considered
Fuzzy PID [24]	MIF	GBSV	based on bang-bang(ON-OFF) method	good tracking performance	more sensitive to disturbances and parametric variations
MPC [25]	MIF, CFS	CQ, MO	based on cross-coupled multivariable structure	effect of the tuning changes are evaluated in real-time, good tracking performance	stability is not guaranteed for parametric variations
Nonlinear MPC [26]	WSPS, MIF	MO, CQ	particle filter, and algebraic routine are used for state estimation	independent control of the variables	large time to solve optimization problem, more computational cost
Nonlinear predictive control [27]	MIF, CFS	MO, MDL	linear quadratic based control law	suitable for MIMO systems	input/output perturbations not considered
Data-driven on-line control [15]	MBT, DP, OT	GBSV	based on process knowledge and operator experience	good regulation performance	difficult to rely on MBT, DP and OT, because these parameters will be affected by mill input variables

TABLE 3. Main VRM process technical parameters and statistical measures.

Process variable	Range	Mean	Standard deviation	Before pre-processing		After pre-processing	
				Skewness	Kurtosis	Skewness	Kurtosis
MIF (tph)	230-370	307	50.297	-0.436	-1.434	-0.449	-1.412
OT (^oC)	75-130	87	4.202	-0.553	-0.966	-0.520	-0.998
DP (mmWC)	200-350	234	42.774	0.854	-0.382	0.397	-0.087
GBBV (mm/s)	0.3-1	0.63	0.066	-0.147	4.628	-2.158	21.087
GBSV (mm/s)	1.5-5	2.5	0.214	-1.490	14.314	-2.497	20.412
GBBDV (mm/s)	5-15	7.8	2.017	0.629	0.659	0.123	-0.080
WSPS (ltr/h)	10000-18000	15637	1610.098	-0.494	1.975	0.052	2.216
MBT (mm)	15-35	23.9	8.146	7.765	15.197	0.567	1.294
TP (bar)	65-150	107	11.462	0.624	-0.643	0.719	-0.888
MFS (rpm)	750-950	869	36.001	0.363	0.558	0.527	0.002
BFS (rpm)	100-3000	544	269.839	-0.340	-1.784	-0.384	-1.777
CFS (rpm)	50-80	67	9.565	0.619	-1.124	0.595	-1.162
RDP (%)	40-70	57	12.077	0.930	-0.375	0.902	-0.400
TMPC (kw)	6500-8500	7361	521.730	-0.166	4.943	-1.112	9.781
SPC (kw/tc)	20.5-30.5	24.6	4.961	0.456	-1.399	0.440	-1.525
MO (tph)	230-370	303	50.297	-0.436	-1.434	-0.449	-1.412

TABLE 4. Correlation coefficient values between different input and output variables of the VRM process.

Variable name	OT (^oC)	DP (mmWC)	GBBV (mm/s)	GBSV (mm/s)	GBBDV (mm/s)	MBT (mm)
MIF (tph)	0.8635	-0.4867	-0.0844	-0.3872	0.3106	-0.0977
WSPS (rpm)	-0.4451	0.6816	0.1765	0.5018	-0.2543	-0.0889
TP (bar)	-0.6189	0.8030	0.0054	0.4224	-0.4039	0.1014
MFS (rpm)	-0.1792	0.6669	-0.3046	0.0762	-0.432	0.3464
BFS (rpm)	0.8486	-0.7284	-0.0596	-0.4627	0.3386	-0.0879
CFS (rpm)	-0.8881	0.5746	0.2497	0.5714	-0.1850	-0.0074

ash 26%, and raw mix 8%. The main technical parameters, their means, and ranges of VRM to produce 230 tph-370 tph PPC are listed in Table 3. These process variables are based on the control expertise and availability to further use the controlling process. The sampling time for collected working plant data is 1 s, and no input delay is considered. TP and BFS are selected as input variables, while OT and DP are responses from the collected real-time data using correlation coefficient values and are shown in Table 4. Skewness and Kurtosis statistical measures provide that the collected data is well enough for system modeling around its mean for the selected process variables. In the preprocessing stage,

TABLE 5. Different design parameters used in the preprocessing.

Preprocessing method	Formula	Design parametrs
Normalization	$x_{normalized} = (x - x_{min})/(x_{max} - x_{min})$	data is normalized between 0 and 1
Moving average filter	$y[n] = (1/M) \sum_{k=0}^{M-1} x(n-k)$	M (window size)=5
Means and trends removal	$x_{detrend} = x - \bar{x}$	mean ($\bar{x}$) values are listed in Table 3

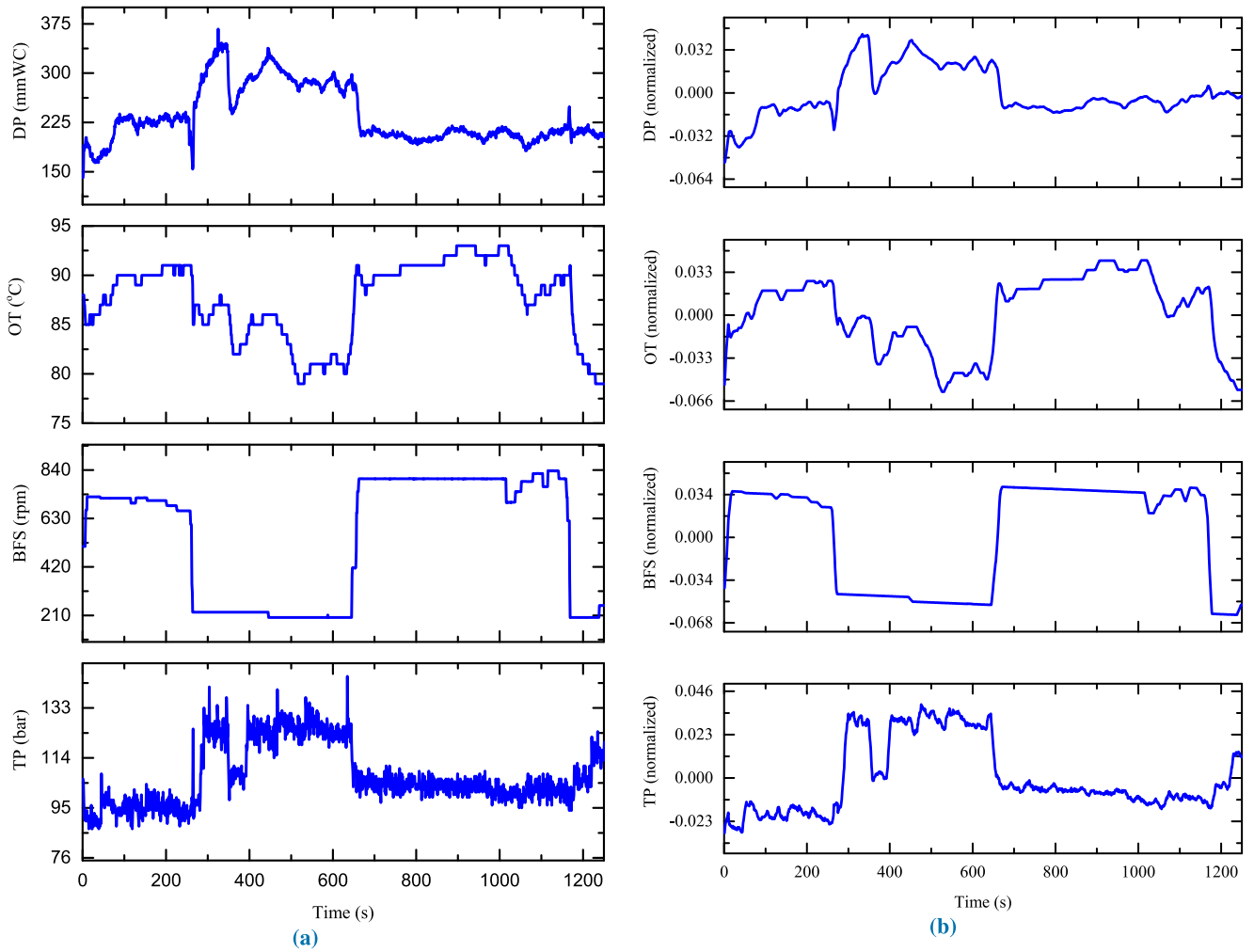

FIGURE 4. Data collected from the cement mill (a) Raw data (b) Preprocessed data.

the data is normalized first, and then a moving average filter is applied; finally, means and trends are removed. Different design parameters used for preprocessing in this work are presented in Table 5.

In Fig. 4, the collected raw data and the data derived after preprocessing for the responses OT and DP concerning inputs BFS and TP are shown.

B. SYSTEM IDENTIFICATION

There are numerous data-based modeling methods available to model complex systems. The generally used time-series data-based modeling methods are transfer function, state-space, process, polynomial and nonlinear methods. The data-based model identification flow diagram is shown in Fig. 5. The empirical or data-based system identification method involves the following entities [29]:

Entity 1: The data, more informative data either by experimenting or collecting the data from the regular operation of the plant, is to be selected.

Entity 2: The set-off candidate models are selected with some unknown parameters using basic physical laws and well-established relationships between the parameters. The better choice is to use standard linear models like transfer function, state-space, polynomial, process, and correlation models.

Entity 3: The best model is determined from the set, based on fit percentage and error metrics; also, the model quality is assessed based on the reproduction of measured data.

TABLE 6. Evaluation of various error metrics of predicted models.

Model	MSE	FPE	AIC	BIC
TF	1.27×10^{-4}	2.26×10^{-9}	-1.97×10^{4}	-1.95×10^{4}
SS	$\mathbf{2.12\times10^{-7}}$	$\mathbf{1.16\times10^{-14}}$	$\mathbf{-3.54\times10^{4}}$	$\mathbf{-3.53\times10^{4}}$
PD	2.25×10^{-4}	7.14×10^{-9}	-1.82×10^{4}	-1.81×10^{4}
ARX	2.18×10^{-7}	1.20×10^{-14}	-3.54×10^{4}	-3.53×10^{4}
ARMAX	2.48×10^{-7}	1.58×10^{-14}	-3.50×10^{4}	-3.49×10^{4}
OE	3.8×10^{-4}	1.31×10^{-8}	-1.74×10^{4}	-1.73×10^{4}
BJ	2.17×10^{-7}	1.21×10^{-4}	-3.54×10^{4}	-3.52×10^{4}
NLARX	1.42×10^{-6}	1.52×10^{-14}	-2.61×10^{4}	-2.59×10^{4}
NLHW	8.29×10^{-4}	6.46×10^{-8}	-1.53×10^{4}	-1.48×10^{4}

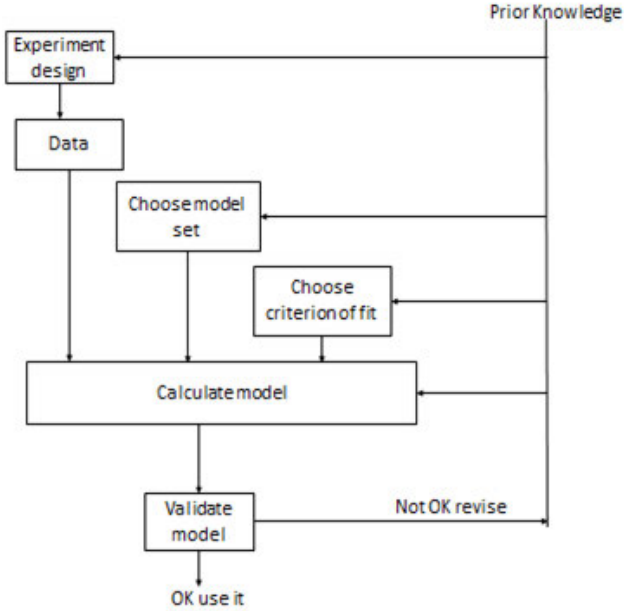

FIGURE 5. Data based system identification process flow.

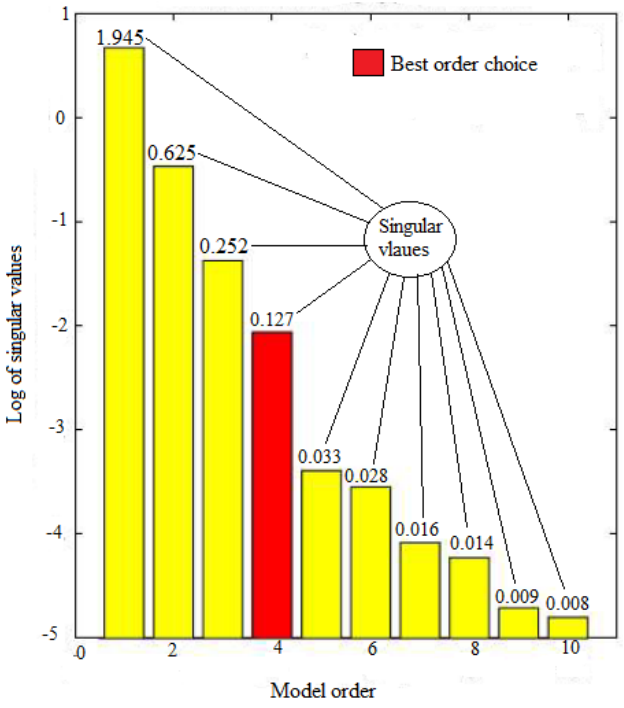

FIGURE 6. State-space model order selection criteria.

Entity 4: Model validation can be carried out using different data sets, which differs from estimating data to evaluate the model properties. Deficient model behavior rejects the model, while good performance will develop absolute confidence in the model.

The identified mathematical models with their percentage fit, MSE, FPE, AIC, and BIC are shown in Table 6. AIC and BIC offer the best fit model to estimate or predict future variables' behavior [30]. The order of the SS model is selected based on the singular values. In Fig. 6, states 3 and 4 provide the most significant contribution. However, the contribution of the states to the right of state 4 drops significantly. This drop indicates that order 4 is sufficient to acquire a good model.

1) STATE-SPACE MODEL STRUCTURE

The generalized form of the continuous-time SS model without feedback is expressed using (1).

$$\begin{aligned} \dot{X}(t) &= AX(t) + BU(t) \\ Y(t) &= CX(t) + DU(t) \end{aligned} \tag{1}$$

where A is $n \times n$ state matrix, B is $n \times m$ cause matrix, C is $l \times n$ response matrix, D is $l \times m$ direct transmission matrix (without feed through D is a zero matrix), $U(t)$ is cause vector, $X(t)$ is the state vector, $Y(t)$ is the response vector, and t is the time [31], [32].

2) POLYNOMIAL MODEL STRUCTURE

The widely used polynomial models are ARX, ARMAX, OE, and BJ [33]–[35]. The general representation of the polynomial model is represented using (2)

$$A(q)y(t) = \sum_{i=1}^{m} \frac{B_i(q)}{F_i(q)} u_i(t - nk_i) + \frac{C(q)}{D(q)} e(t) \tag{2}$$

where u_i is i^{th} input, nk_i is i^{th} input delay, $e(t)$ is noise variance, $A(q), B(q), C(q), D(q)$, and $F(q)$ are the polynomials in the time shift operator q.

In most cases, linear identification methods produce satisfactory models. For complex nonlinear systems, linear models are sometimes not suitable for handling the system's dynamics, then nonlinear modeling methods

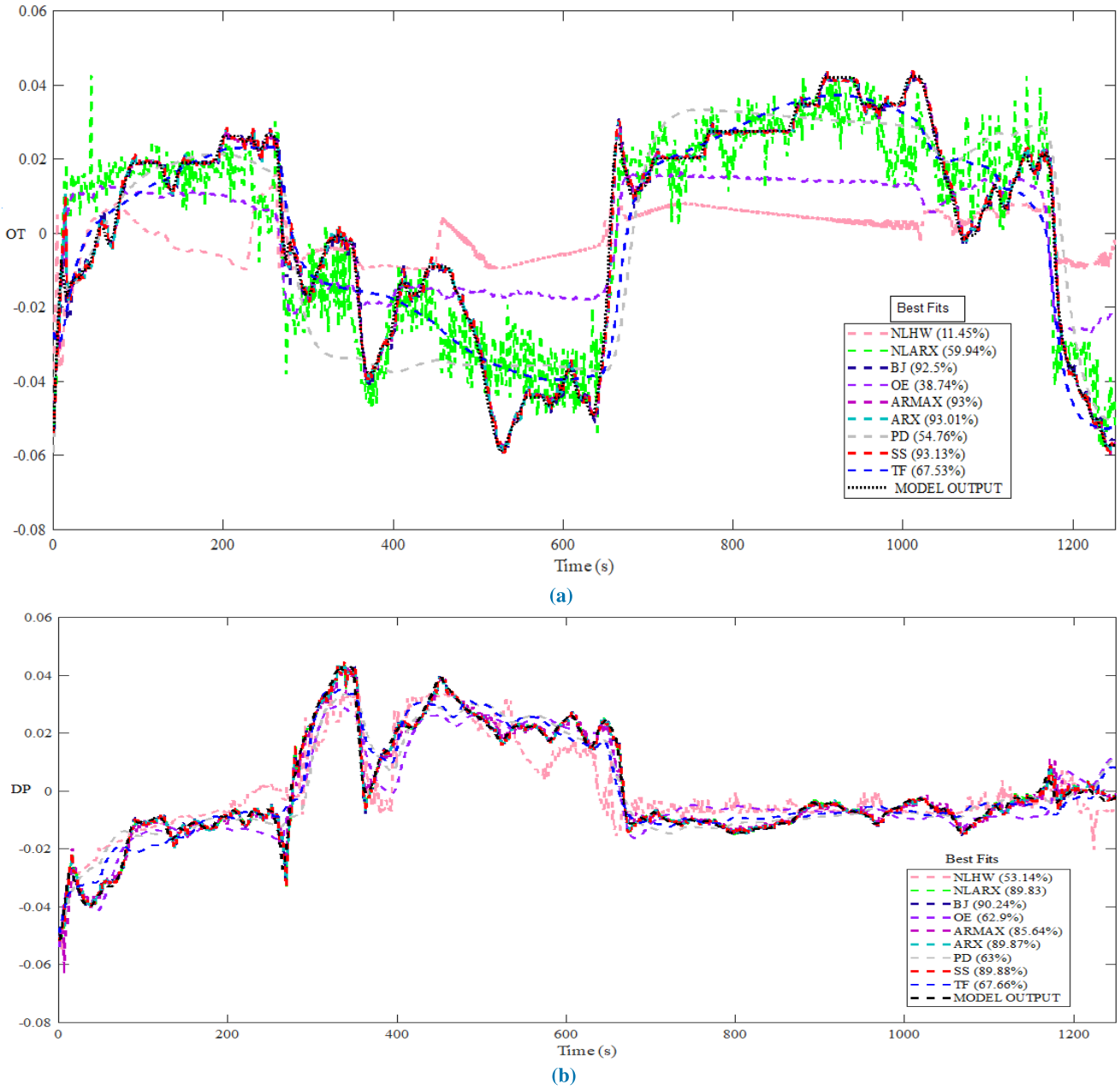

FIGURE 7. The model fit percentage using different system identification methods (a) for OT (b) for DP.

like nonlinear ARX and Hammerstein-Wiener models are preferred [28], [31]. From Fig. 7 and Table 6, SS modeling gives the best fit mathematical model with fit percentages 93.13 and 89.88 for OT and DP, respectively. In Fig. 8, the predicted error for the SS model is shown. The obtained VRM model with order four using the SS method is represented as:

$$A = \begin{bmatrix} 0.1845 & 0.0758 & 0.2266 & 0.1304 \\ 0.0451 & 0.0871 & -0.0702 & 0.4175 \\ -0.2477 & -0.1152 & -0.2502 & -0.283 \\ -0.0906 & -0.1065 & -0.0276 & -0.3155 \end{bmatrix}$$

$$B = \begin{bmatrix} -0.0361 & 0.0893 \\ -0.1453 & 0.1004 \\ 0.1064 & -0.1199 \\ 0.0694 & -0.0581 \end{bmatrix}$$

$$C = \begin{bmatrix} 0.5413 & 0.1028 & 0.0506 & 0.0840 \\ 0.1797 & -0.2819 & 0.0398 & -0.0615 \end{bmatrix}$$

$$D = \begin{bmatrix} 0 & 0 \\ 0 & 0 \end{bmatrix}$$

The flexibility to adapt to advanced control methods makes the SS modeling is the right choice in system identification [31], [32].

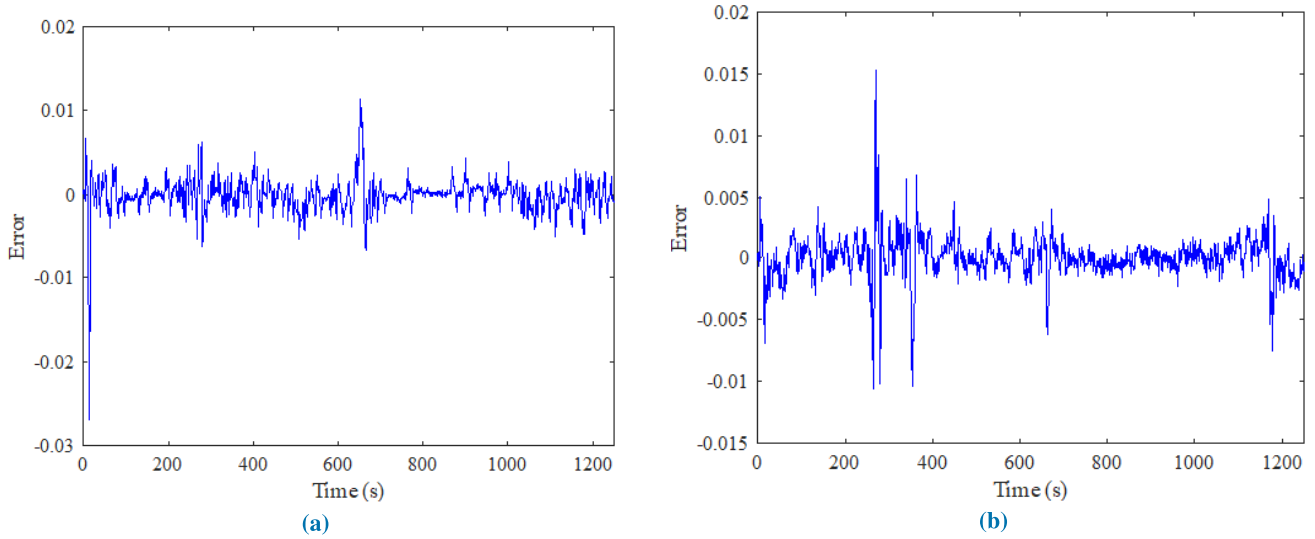

FIGURE 8. Predicted model error (a) for OT (b) for DP.

III. PROCESS CONTROL

Efficiency improvement, output optimization, and to keep investment cost minimum; the proper control of VRM is desirable. The control objective is to maintain the DP and OT at desired values by manipulating the BFS and TP. The disturbance signals like inlet feed, classifier speed, mill vibrations, etc., cause parametric changes. Hence, set-point tracking and disturbance rejection are needed while the plant is running. In multi-variable systems, the interaction between the control loops is measured using RGA to provide the best input-output variable pairing [36]. The RGA results obtained using BFS, TP as inputs and OT, DP as outputs are $\begin{bmatrix} 1.0975 & -0.0975 \\ -0.0975 & 1.0975 \end{bmatrix}$.

From the RGA matrix, the interaction of the loops TP-OT and BFS-DP is robust; hence, these loops are used to design the controller for the VRM.

A. PI CONTROL

In most of the cement mills, PI control is considered as the traditional one. The mathematical representation of the PI control law is:

$$u(t) = K_p e(t) + K_i \int_0^t e(t)dt \tag{3}$$

where K_p and K_i are non-negative proportional and integral terms, respectively.

The Derivative action is made zero because of its variable impact on the stability of the system. The block diagram of the PI controller for VRM is shown in Fig. 10a. PI tuning and control law implementation advancements made it a widely used method for many simple MIMO systems. Adaptive PI control implementation gives good performance for parametric variations and disturbance rejection for many linear time-invariant systems. However, the inability to handle slow disturbance effects, design complexity for higher-order systems, the implementation for optimal control problems, and constraints governing capability limit it's application [37], [38].

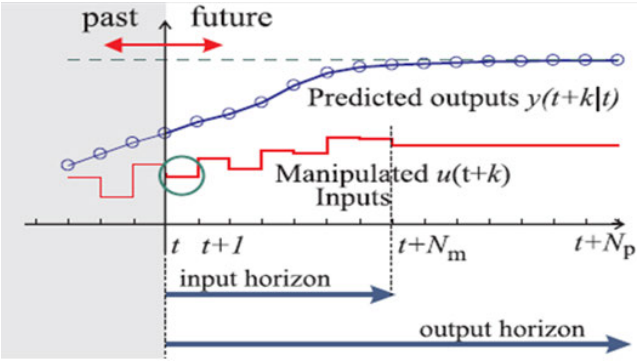

FIGURE 9. Process diagram of receding horizon control.

B. MODEL PREDICTIVE CONTROL

Most traditional control methods do not consider the process's knowledge, therefore compromising the set-point tracking and disturbance rejection accuracy. Also, classical controllers do not guarantee the set-point tracking for higher-order dynamic and time delay processes. MPC control is preferred for such type of systems. MPC control scheme uses a model to predict the plant's future behavior by optimizing the control signal. Fig. 9 represents the receding horizon MPC controller process flow diagram. The optimized control signal at each sampling instant is applied to the system. Then, at time $t + 1$, a new control law is generated by solving the optimal control problem. In MPC, only the first step control strategy is implemented, and then the plant state is sampled again, and from the new current state, the calculations are repeated. The prediction horizon keeps being shifted forward. The feedback information is collected from the plant at each sampling instant to improve

it's desired performance. Nowadays, most industries try to adapt the MPC control method to satisfy the various constraints without compromising the set-point tracking and disturbance rejection. It anticipates future events and takes necessary control actions, which are not reliable using traditional control methods. The steady value information to track the set-point and solve the optimization problem in MPC is essential. The exact steady-state value is not possible because of the system's uncertainty [22], [38]. The handling capacity of complex interacting sub-systems in a plant is difficult to control by the centralized MPC, but decentralized MPC is started for such types of systems [39]. In this wok, decentralized MPC is considered for the VRM process. The block diagram of the MPC controller for VRM is shown in Fig. 10b. The MPC controller's main limitations include the necessity of accurate model, optimization algorithm, high computational cost, difficulty to resolve uncertainty problems, and no guarantee in its stability for higher-order systems.

C. ADAPTIVE MODEL PREDICTIVE CONTROL

The modern control methods provide better control action to stabilize the response without considering the working plant's parametric variations. The AMPC updates the prediction model for a single controller as operating conditions changes. This control only needs to design a single controller; therefore, less run-time computational effort and a smaller memory footprint for more robust changes in plant conditions. Hence, an adaptive MPC controller can handle the parametric variations without compromising the plant's closed-loop stability [40]. To achieve the control objective for two different variables OT and DP, DAMPC is proposed in this research work. Fig. 10c shows the proposed DAMPC block diagram for the VRM process.

The algorithmic steps involved in AMPC design are described as follows:

Step 1: Acquire the measurement

Step 2: Evaluate the uncertain parameters

Step 3: Compute the updated MPC control law with the estimated model

Step 4: Apply the MPC law and go to step 1

In this research work, parameters are estimated on-line for the polynomial ARX model. The model is then converted into the SS model because of the identified plant model in state space. In the following subsections, the formulation of DAMPC is proceeded [39], [41]–[44].

1) ON-LINE PARAMETER ESTIMATION FOR ARX MODEL

The same VRM grinding machine is used to produce different cement types by changing the machine's input parameters; these changes cause closed-loop instability and poor tracking performance. The identified SS model parameters (A, B, C, and D) are estimated on-line using a recursive polynomial estimator in this work [45], [46]. The dynamics of the SISO system may capture accurately by estimating the relatively large number of model parameters when subjected

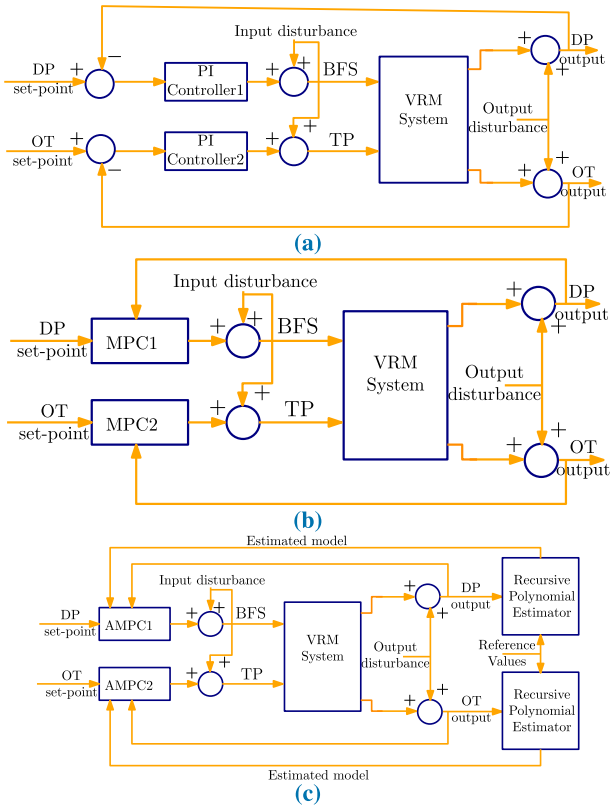

FIGURE 10. Block diagram of VRM process control with disturbance signals using (a) PI control, (b) MPC control, (c) Adaptive MPC control.

to disturbances. The changes in errors are reduced with large data set, which complicates the on-line parameter estimation. Hence, higher-order models are required to accurately capture the dynamics, which leads to difficulty in the controller's design using on-line parameter estimation. The plant needs to be perturbated for a longer time to estimate the parameters more precisely. This difficulty is further extended to the MIMO system. A feasible solution to overcome on-line parameter estimation for the MIMO system is to use polynomial MISO models [47]–[49]. Consider a MIMO system with n-outputs and m-manipulated inputs. The system is linearized at the desired operating point such that the linear model is invertible and stable. The MIMO system in this work is spitted into n-Multi-input single-output (MISO) ARX models and expressed as:

$$A_i(q^{-1})y_i(k) = \sum_{j=1}^{m} B_{ij}(q^{-1})u_j(k) + e_i(k) \tag{4}$$

where $i = 1, 2, \ldots.., n$, q^{-1} is backward shift operator, $e_i(k)$ is zero- mean white noise, $A_i(q^{-1})$, and $B_{ij}(q^{-1})$ are polynomials in backward shift operator q^{-1}.

The n^{th} MISO model is expressed using (5) (i-is omitted to reduce the complexity).

$$A(q^{-1})y(k) = \sum_{j=1}^{m} B_j(q^{-1})u_j(k) + e(k) \tag{5}$$

For on-line parameter estimation (5) is represented as:

$$y(k) = \phi^T(k-1)\theta(k-1) + e(k) \tag{6}$$

where θ and ϕ are model parameters and regressor vectors, represented using (7) and (8), respectively.

$$\theta = [a_1, \ldots, a_n, b_{11}, \ldots, b_{m1}, \ldots, b_{mn}]^T \tag{7}$$

$$\phi(k-1) = [-y(k-1), \ldots, -y(k-n), u_1(k-1), \ldots, u_m(k-n), e(k-1), \ldots, e(k-n)]^T \tag{8}$$

The difficulty with the regressor vector to use in recursive parameter estimation is that the noise sequence $e(k)$ is unknown. This problem is addressed by using the ELS method. In this paper, $e(k)$ is replaced with the estimated prediction error using the ELS method. The regressor vector using the ELS approach is then modified as:

$$\phi(k-1) = [-y(k-1), \ldots, -y(k-n), u_1(k-1), \ldots, u_m(k-n), \epsilon(k-1), \ldots, \epsilon(k-n)]^T \tag{9}$$

In this, $e(k-n)$ is replaced with the $\epsilon(k-n)$, which is the past innovations. The $\epsilon(k)$ at instant k is represented as:

$$\epsilon(k) = y(k) - \phi^T(k-1)\hat{\theta}(k-1) \tag{10}$$

where $\hat{\theta}(k-1)$ represents the parameter estimate at an instant $(k-1)$. The ELS algorithm is summarized as:

$$\hat{\theta}(k) = \hat{\theta}(k-1) + L(k)\epsilon(k) \tag{11}$$

$$L(k) = P(k-1)\phi(k-1)(\lambda + \phi^T(k-1)P(k-1) * \phi(k-1))^{-1} \tag{12}$$

$$P(k) = (I - L(k)\phi^T(k-1))P(k-1)/\lambda \tag{13}$$

where $L(k)$ is the Kalman gain matrix, $P(k)$ is the covariance matrix, and λ is the forgetting factor.

In this paper, n-MISO recursive polynomial estimators used to identify the model, i.e., $\hat{\theta}^{(i)}(k)$ and $P^{(i)}(k)$ for $i = 1, 2, 3 \ldots n$, are estimated and used in the DMPC formulation. One step ahead prediction for the model is represented as:

$$\hat{y}_i(k+1) = \mathbb{E}[y_i(k+1)|Y(k)] = [\phi^{(i)}(k)]^T\hat{\theta}^{(i)}(k) \tag{14}$$

where $Y(k)$ is the set of input and output data collected from the plant, $\mathbb{E}$ is the expected operator. The convergence of the ELS estimates to the true parameters implies that the $\epsilon(k)$ asymptotically converges to $e(k)$.

2) THE COST FUNCTION FOR DAMPC

The objective of the DAMPC is to find the optimal control sequences to minimize the cost function represented in equation below.

$$J_\infty = \mathbb{E}\left\{\sum_{j=k+1}^{\infty}\left[\sum_{i=1}^{n} w_i E_i(j)^2 + \sum_{i=1}^{m}\mu_i u_i(j-1)^2\right]|Y(k)\right\} \tag{15}$$

where $E_i(j) = r_i(j) - y_i(j)$, $w_i > 0$ and $\mu_i \geq 0$ are the weighting parameters and $r(j)$ is the reference vector. When μ_i is too large, the cost function is dominated by the control effort u, and so the controller minimizes the control action itself. With the overlooked control effort by u, the system's gain will go to zero so that the closed-loop poles approach to open-loop poles may cause closed-loop instability. In VRM process control, the main focus is on reference tracking by minimizing the error values. The large value of prediction horizon N_P is not the problem in stable and invertible systems; therefore, μ_i is considered zero. The cost function then becomes

$$J_\infty = \mathbb{E}\left\{\sum_{j=k+1}^{\infty}\left[\sum_{i=1}^{n} w_i E_i(j)^2\right]|Y(k)\right\} \tag{16}$$

The cost function is reformulated subjected to the model designed as:

$$J_\infty = \mathbb{E}\left\{\sum_{j=k+1}^{k+2}\left[\sum_{i=1}^{n} w_i E_i(j)^2\right]|Y(k)\right\} + \mathbb{E}\left\{\sum_{j=k+3}^{\infty}\left[\sum_{i=1}^{n} w_i E_i(j)^2\right]|Y(k)\right\} \tag{17}$$

Consider the first term,

$$J_1 = \sum_{i=1}^{n} w_i J_{1i} \tag{18}$$

where

$$J_{1i} = \mathbb{E}\left\{E_i(k+1)^2|Y(k)\right\} \tag{19}$$

By adding and subtracting the model $\hat{y}_i(k+1)$, equation (19) can be written as

$$J_{1i} = \mathbb{E}\left\{(r_i(k+1) - \hat{y}_i(k+1) + \delta y_i(k+1))^2|Y(k)\right\} \tag{20}$$

where

$$\delta y_i(k+1) = \hat{y}_i(k+1) - y_i(k+1) \tag{21}$$

By dropping the conditional expectation $|Y(k)$ for the sake of simplicity, the equation (21) is expressed as

$$J_{1i} = \mathbb{E}\{(r_i(k+1) - \hat{y}_i(k+1))^2 + (\delta y_i(k+1))^2 - 2(r_i(k+1) - \hat{y}_i(k+1))(\delta y_i(k+1))\} \tag{22}$$

where

$$\delta y_i(k+1) = [\phi^{(i)}(k)]^T\delta\theta^{(i)}(k) \tag{23}$$

and

$$\delta\theta^{(i)}(k) = \hat{\theta}^{(i)}(k) - \theta^{(i)}(k) \tag{24}$$

The equation (22) can be re-written as

$$J_{1i} = \mathbb{E}\big[(r_i(k+1) - \hat{y}_i(k+1))\big]^2 + \mathbb{E}\big[(\delta y_i(k+1))\big]^2 - \mathbb{E}\big[2(r_i(k+1) - \hat{y}_i(k+1))(\delta y_i(k+1))\big] \tag{25}$$

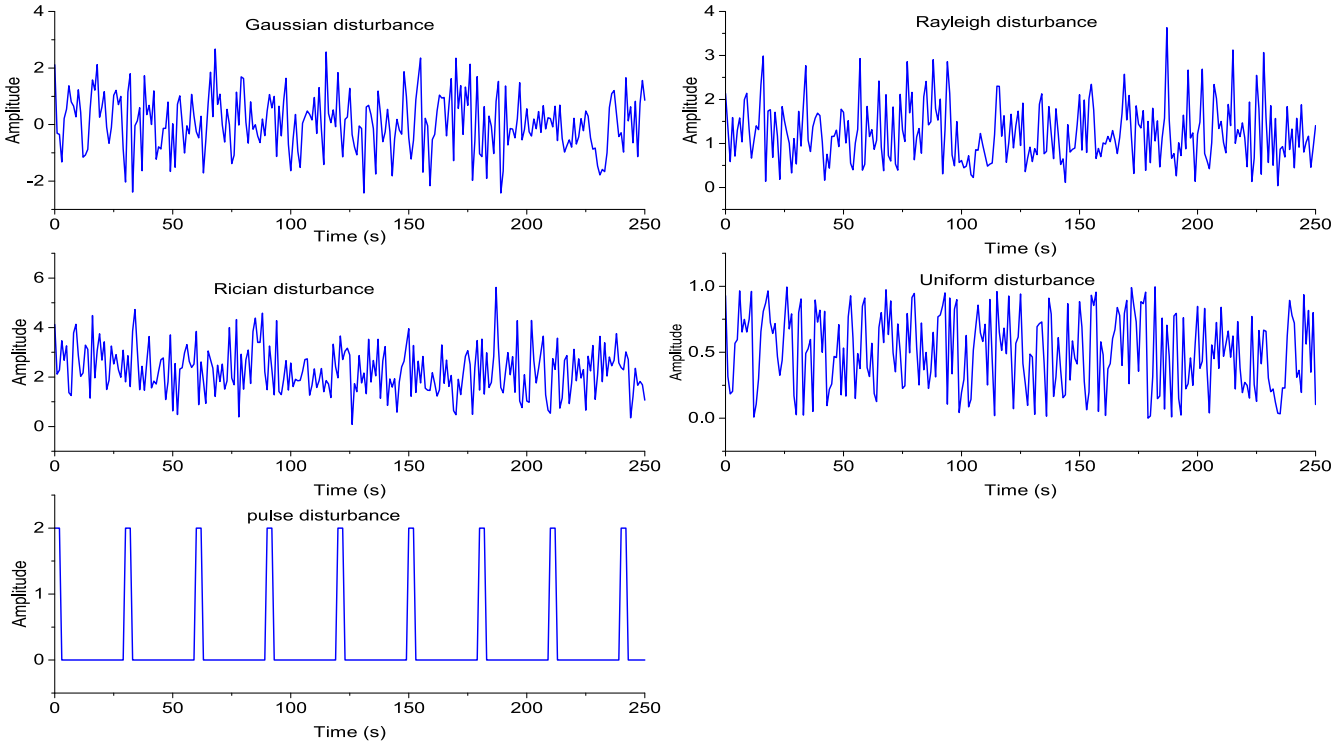

FIGURE 11. Responses of different disturbance signals.

By using (14) and (23), the above equation can be written as

$$\begin{aligned} J_{1i} &= \mathbb{E}\left[(r_i(k+1) - [\phi^{(i)}(k)]^T \hat{\theta}^{(i)}(k))\right]^2 \\ &+ \mathbb{E}\left[([\phi^{(i)}(k)]^T \delta\theta^{(i)}(k))\right]^2 \\ &- \mathbb{E}\left[2(r_i(k+1) - [\phi^{(i)}(k)]^T \hat{\theta}^{(i)}(k)) \right. \\ &\left. ([\phi^{(i)}(k)]^T \delta\theta^{(i)}(k))\right] \end{aligned} \tag{26}$$

By applying the expectation operator to individual terms

$$\begin{aligned} J_{1i} &= \mathbb{E}\left[(r_i(k+1) - [\phi^{(i)}(k)]^T \hat{\theta}^{(i)}(k))\right]^2 \\ &+ \mathbb{E}\left[([\phi^{(i)}(k)]^T \delta\theta^{(i)}(k))\right]^2 \\ &- 2\mathbb{E}\left[(r_i(k+1) - [\phi^{(i)}(k)]^T \hat{\theta}^{(i)}(k)\right] \\ &\mathbb{E}\left[[\phi^{(i)}(k)]^T \delta\theta^{(i)}(k)\right] \end{aligned} \tag{27}$$

Since, ELS algorithm is assumed to be asymptotically unbiased estimator, i.e.,

$$\mathbb{E}\left\{\delta\theta^{(i)}(k)\right\} = 0 \tag{28}$$

By substituting (28) in (27),

$$\begin{aligned} J_{1i} = \mathbb{E}\left[(r_i(k+1) - [\phi^{(i)}(k)]^T \hat{\theta}^{(i)}(k))\right]^2 \\ + \mathbb{E}\left[([\phi^{(i)}(k)]^T \delta\theta^{(i)}(k))\right]^2 \end{aligned} \tag{29}$$

By assuming $cov[\delta\theta^{(i)}(k)] = P^{(i)}(k)$ and evaluating the expected operator, (29) can be written as

$$J_{1i} = \left[r_i(k+1) - [\phi^{(i)}(k)]^T \hat{\theta}^{(i)}(k)\right]^2 + [\phi^{(i)}(k)]^T P^{(i)}(k) \phi^{(i)}(k) \tag{30}$$

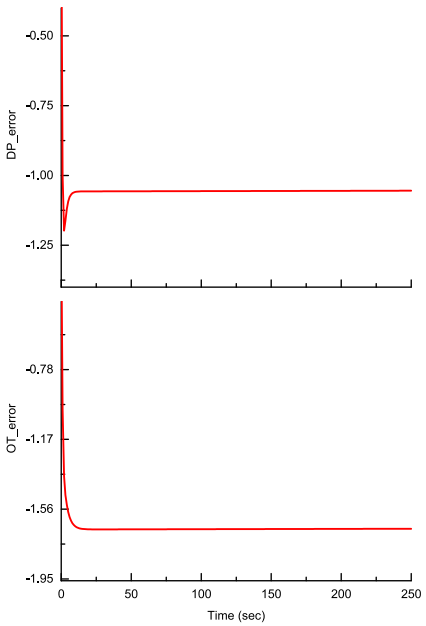

FIGURE 12. Output prediction error using a Recursive polynomial model estimator.

Similarly,

$$\begin{aligned} J_{2i} = \left[r_i(k+2) - [\phi^{(i)}(k+1)]^T \hat{\theta}^{(i)}(k+1)\right]^2 \\ + [\phi^{(i)}(k+1)]^T P^{(i)}(k+1) \phi^{(i)}(k+1) \end{aligned} \tag{31}$$

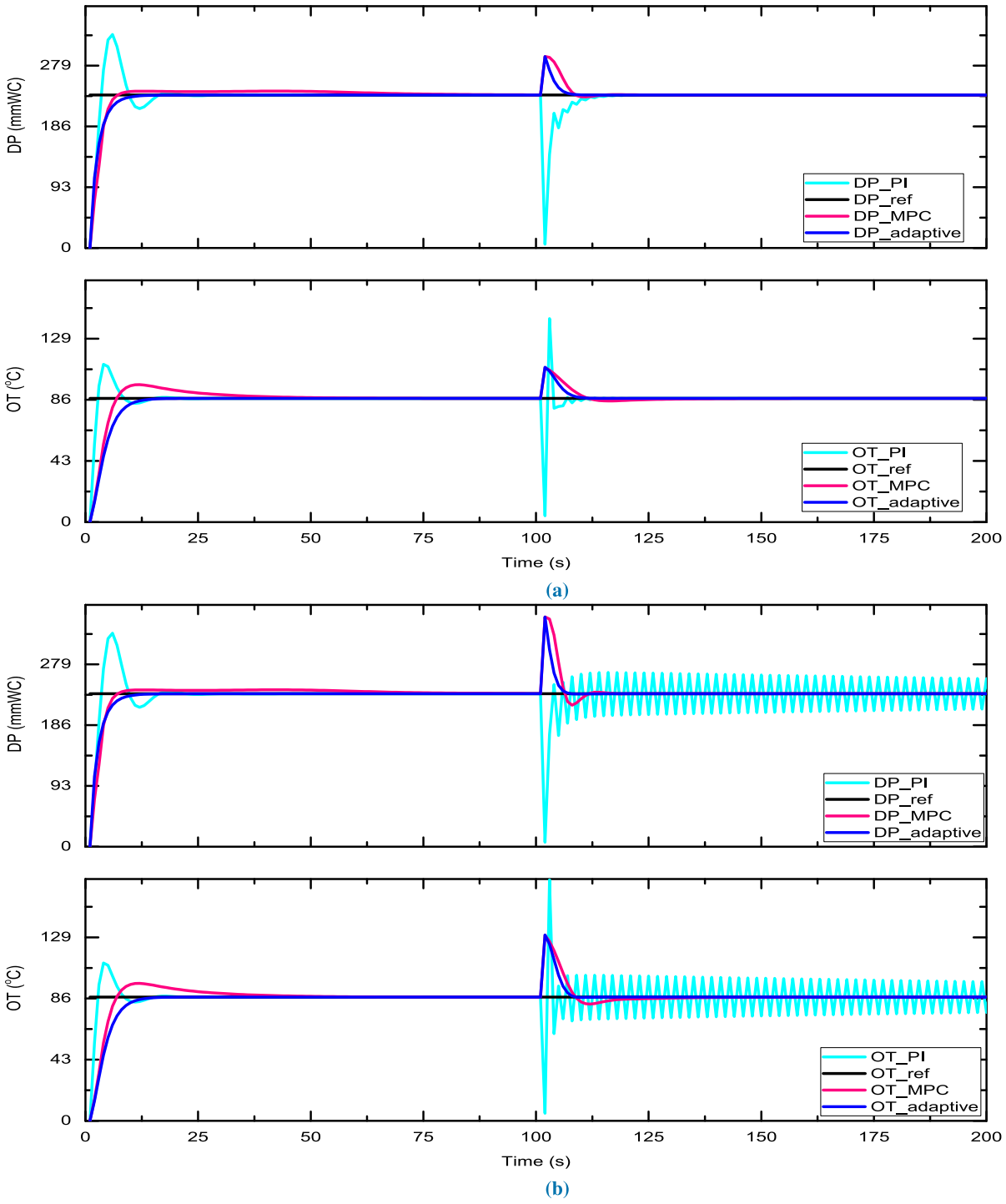

FIGURE 13. Effect of parametric variations on the dynamic response of different control systems (a) for 25% increase in gain(b) for 50% increase in gain.

By truncating the infinite horizon to finite number N, J_∞ can be expressed as

$$J_N \simeq \sum_{j=k}^{k+1}\sum_{i=1}^{n}\left[w_i\left(r_i(j+1)-[\phi^{(i)}(j)]^T\theta^{(i)}(j)\right)^2 + w_i\left([\phi^{(i)}(j)]^T P^{(i))}(j)\phi^{(i)}(j)\right)\right]$$

$$+\mathbb{E}\left\{\sum_{j=k+2}^{k+N}\sum_{i=1}^{n}\left[w_i(E_i(j+1))^2\right]\right\}|Y(k) \qquad (32)$$

After replacing the expected values with model prediction, (32) is expressed as:

$$V_N = \sum_{j=k}^{k+1}\sum_{i=1}^{n}\left[w_i\left(r_i(j+1)-[\phi^{(i)}(j)]^T\theta^{(i)}(j)\right)^2\right.$$

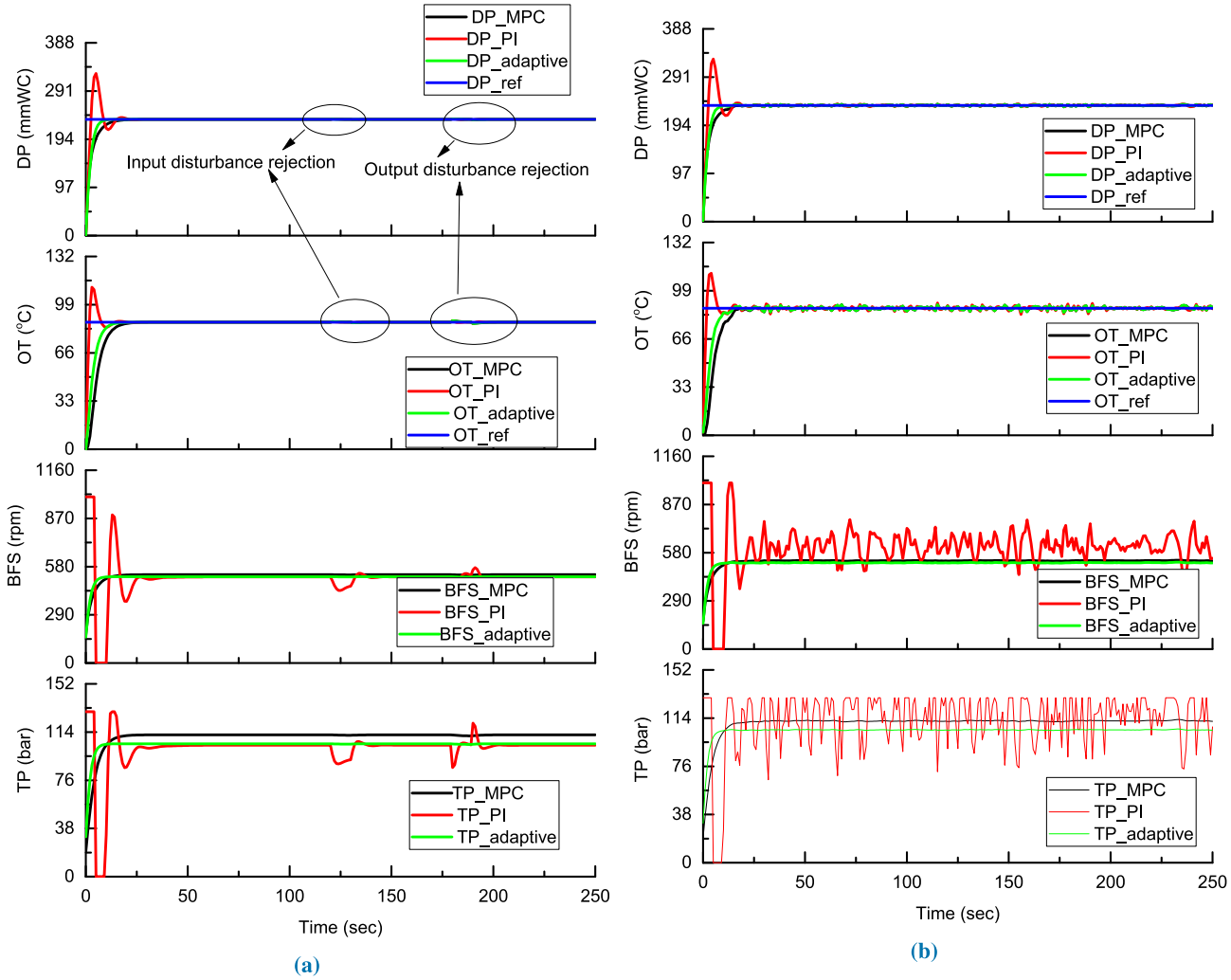

FIGURE 14. Disturbance rejection and reference tracking with different disturbances (a) step (b) pulse.

$$+ w_i\Big([\phi^{(i)}(j)]^T P^{(i)}(j)\phi^{(i)}(j)\Big)\Big] + \sum_{j=k+2}^{k+N}\sum_{i=1}^{n}[w_i\Big(r_i(j+1) - \hat{y}_i(j+1|k)\Big)^2 \quad (33)$$

In equation (33), the covariance matrix $P^{(i)}(k+1)$ and future regressor vector $\phi^{(i)}(k+1)$ are the functions of $u(k)$. As a result, the optimization objective rewards inputs that reduce the future covariance $P^{(i)}(k+1)$. Therefore, the parameter estimate's quality is improved by the insertion of inputs, thereby reducing parameter uncertainty.

3) OUTPUT PREDICTION

In the projected AMPC formulation, the identified models are used to predict future outputs. With the known time k and the probable value of the unknown parameter $\hat{\theta}^{(i)}(k)$ in n^{th}, the model outputs are predicted by using (34).

$$\hat{\theta}^{(i)}(k+j|k) = \hat{\theta}^{(i)}(k) \quad (34)$$

for $j > 0$ and all values of i. The predicted output for the n^{th} MISO ARX model at time $k+j$ is expressed as

$$\hat{y}_i(k+j+1|k) = [\phi^{(i)}(k+j|k)]^T \hat{\theta}^{(i)}(k) \quad (35)$$

where, the predicted regressor vector is represented using (36).

$$\begin{aligned}\phi^{(i)}(k+j|k) = [&\hat{y}_i(k+j|k), \ldots, -\hat{y}_i(k+1|k), -y_i(k),\\ &\ldots\ldots, -y_i(k+j-n+1), u_1(k+j|k), \ldots,\\ &u_m(k+j|k), \ldots, u_m(k+j-n),\\ &u_m(k+j|k), \ldots, u_(k+j-n)]^T\end{aligned} \quad (36)$$

valid for $j = 0, 1, \ldots\ldots, N-1$ and $i = 1, 2, \ldots.., r$(number of parallel MISO estimators). [39], [41].

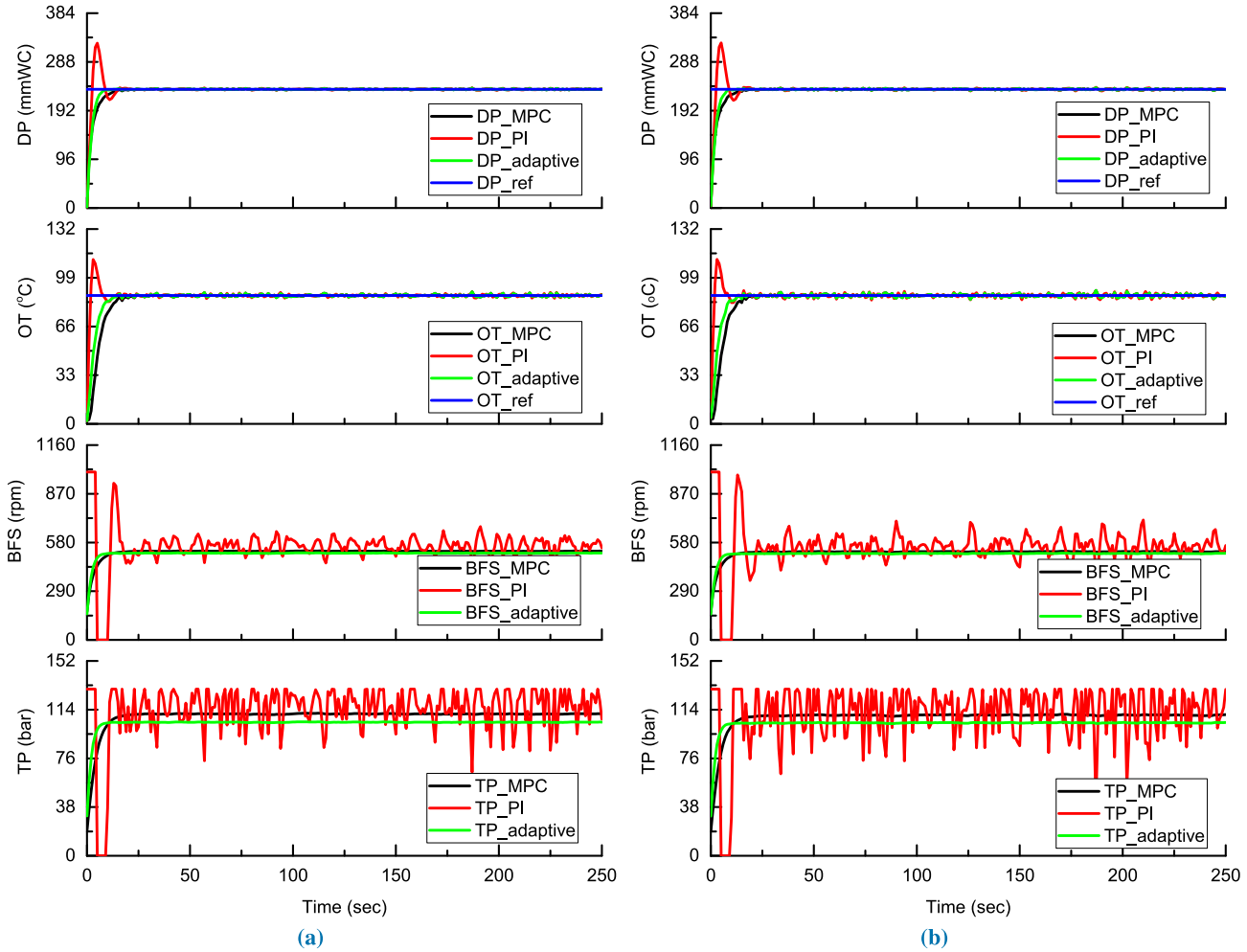

FIGURE 15. Disturbance rejection and reference tracking with different disturbances (a) Gaussian (b) Rayleigh.

4) DAMPC FORMULATION

By using cost function V_N and predicted model $\hat{y}_i(k+j+1|k)$ the DAMPC is formulated as follows

$$\min_{u_k} V_N(k) = \sum_{j=k+1}^{k+N} E(j)^T W_E E(j) + \sum_{j=k}^{k+1} \sum_{i=1}^{n} w_i \left[\phi^{(i)}(j|k)\right]^T P^{(i)}(j)\phi^{(i)}(j|k) + \sum_{j=k+3}^{k+N} \Delta u^T(j) W_{\Delta u} \Delta u(j) \quad (37)$$

where $\Delta u(j) = u(j) - u(j-1)$, $E(j) = r(j) - \hat{y}(j|k)$ and $\hat{y}_i(j|k) = [\phi^{(i)}(j-1|k)]^T \hat{\theta}^{(i)}(k)$ for $i = 1, 2, \ldots n$, subjected to the following constraints

$$P^{(i)}(k+1) = [I - L_i(k+1)\phi^{(i)}(k)]P^{(i)}(k) \quad (38)$$

$$L_i(k+1) = P^{(i)}(k)\phi^{(i)}(k)[1 + \phi^{(i)}(k)^T P^{(i)}(k)\phi^{(i)}(k)]^{-1} \quad (39)$$

$$\Delta u_{min} \leq \Delta u(j) \leq \Delta u_{max} \quad (40)$$

where $\Delta u(j) = 0$ for $j = k + N_c, \ldots, k + N - 1$, N_c is the control horizon, and $W_E = diag[w_1, w_2, \ldots w_n]$ is the tracking error matrix. The weighting matrix $W_{\Delta u}$ is used to counteract massive input changes that can otherwise occur when $P^{(i)}(k)$ is large.

The proposed DAMPC design procedure is summarized with the following algorithmic steps [42], [47], [49]:

Step 1: Initialize the system at time $t = t_0$, and specify the parameters $\phi(t_0)$, $u(t_0 - 1)$, $\hat{\theta}(t_0)$, and $P(t_0)$.

Step 2: At time t collect system data.

Step 3: Measure $y(t)$ and $u(t-1)$ at current time t.

Step 4: Update the parameters $u(t-1)$, and $\phi(t)$.

Step 5: Update the parameters $\hat{\theta}(t)$, and $P(t)$ using the on-line parameter estimation.

Step 6: Apply the AMPC algorithm and obtain the adaptive control law $\left[u^0(k|t)\right]_{k=t}^{t+N-1}$.

Step 7: Implement $u^0(t|t)$.

Step 8: Set $t \leftarrow t + 1$ and go to step 2.

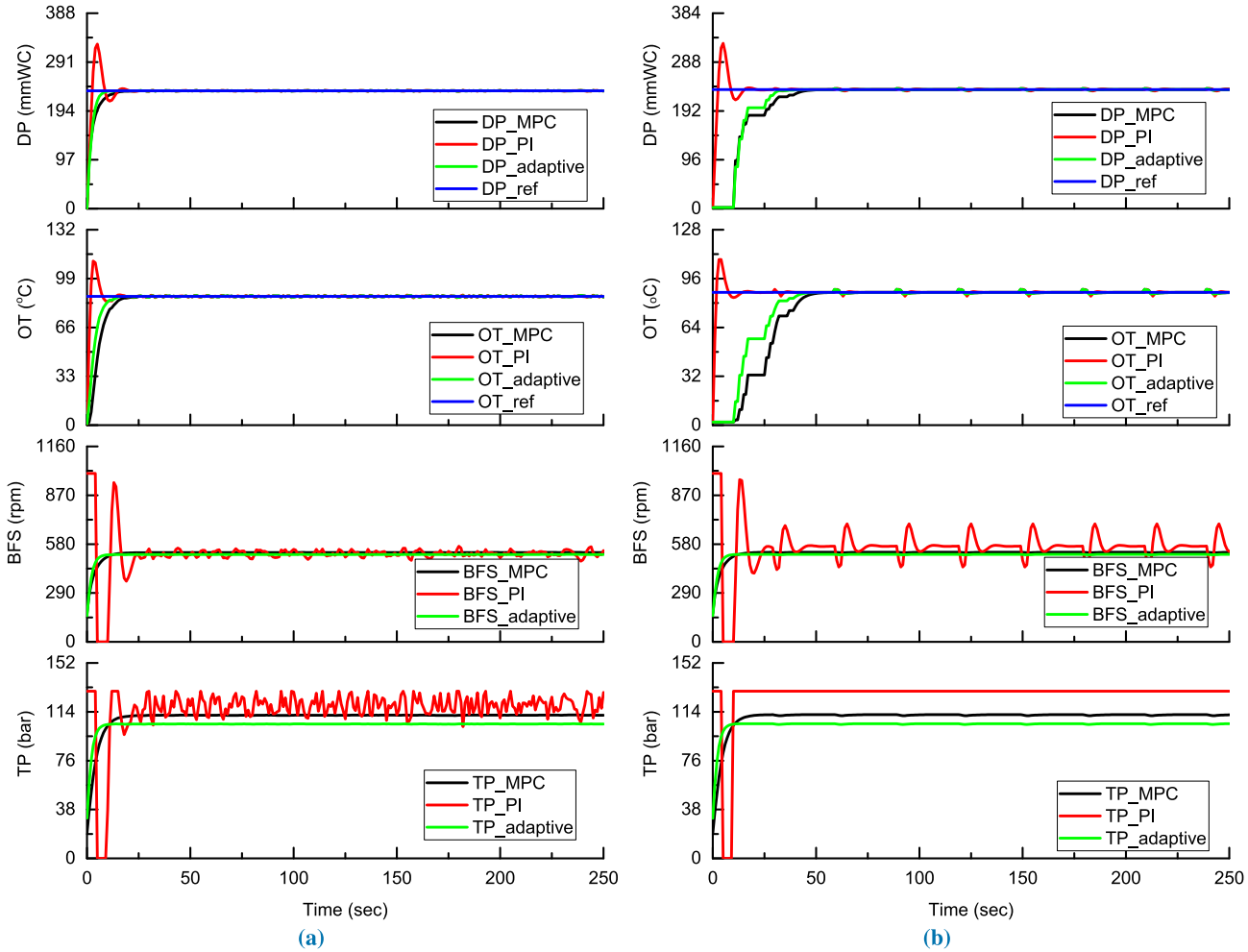

FIGURE 16. Disturbance rejection and reference tracking with different disturbances (a) Rician (b) Uniform.

IV. RESULTS AND DISCUSSION

The optimal operating points considered in this research work are OT = 87 ^oC, DP = 234 mmWC, BFS = 544 rpm and TP = 107 bar. These set-points are selected to produce approximately 310 tph of PPC cement. MATLAB R2019a is used to perform the simulation. The input disturbances mainly due to the variations in inlet feed, and output disturbances are due to the mill vibrations. The parametric variations are considered by applying the plant's different disturbances at the input and output side. These disturbance signals are random; hence, Gaussian, Rayleigh, Rician, Uniform, and Pulsated disturbances are considered in simulation with sampling time 1 s and are shown in Fig. 11. For comparison purposes, the traditional PI controller used in the VRM machine is also designed in this work. PI controller for OT is tuned with ($k_p = 29.386, k_i = 1.103$) using bode analysis with gain margin infinity rad/s and phase margin 55.1 degrees. PI controller for DP is tuned with ($k_p = 12.848, k_i = 0.632$) with gain margin infinity rad/s and phase margin 53.3 degrees. In both the controllers, closed-loop stability is achieved.

Decentralized MPC is designed with a prediction horizon (N) 10 and the control horizon (N_c) 3 with constraints; OT: 75^oC-130 ^oC, DP: 200 mmWC-350 mmWC, BFS: 100 rpm-3000 rpm and TP: 65 bar-150 bar. The controller performance is verified concerning disturbance rejection and reference tracking. The designed MPC controller is adapted in DAMPC with the same constraints and settings. The initial coefficients (Aq, Bq) for the Recursive Polynomial ARX estimator are derived from the numerator and denominator terms from the identified plant model. The prediction error using a recursive estimator is shown in Fig. 12. Initially, the error is large, but it settles at a significantly less value when time progresses. The estimated model parameters are equal to the model identified using the real-time data collected from the plant.

The parametric variations to the closed-loop VRM are applied by increasing the system's gain to 25% and 50%; this is achieved by changing the matrix B value in the identified VRM SS model from an initial 100% to 125% and 150%, respectively. Fig. 13 shows the VRM closed-loop control system's dynamic behavior with parametric variations applied at the 100th s. The existing PI controller performance is abysmal

TABLE 7. Performance evaluation of different controllers.

Disturbance signal	Process variable	Control method	MSE	IAE	ISE	ITAE	ITSE	Over shoot (%)	Rise time (s)	Peak time (s)	Settling time (s)
Step	OT	PI	0.0049	0.2397	0.0739	0.0240	0.0074	25.949	1.0910	2.4890	21.200
		MPC	0.0101	0.5743	0.2041	0.0574	0.0204	-	7.9840	-	17.180
		AMPC	0.0104	0.5157	0.2103	0.0516	0.0210	-	6.7690	-	14.336
	DP	PI	0.0074	0.6366	0.2522	0.0637	0.0252	63.115	1.4820	4.3840	21.209
		MPC	0.0090	0.5560	0.1978	0.0556	0.0198	-	7.8120	-	18.602
		AMPC	0.0074	0.3433	0.1368	0.0343	0.0137	-	4.0170	-	11.019
Pulse	OT	PI	0.0043	0.3042	0.0664	0.0304	0.0066	25.949	1.0950	2.7250	17.654
		MPC	0.0090	0.6827	0.1850	0.0683	0.0185	-	9.7530	-	16.469
		AMPC	0.0092	0.6294	0.1906	0.0629	0.0191	-	7.9610	-	15.758
	DP	PI	0.0100	0.7686	0.2090	0.0769	0.0209	63.110	1.4810	4.3840	18.839
		MPC	0.0088	0.6650	0.1790	0.0666	0.0179	-	9.6230	-	17.654
		AMPC	0.0065	0.4499	0.1229	0.0450	0.0123	-	5.9590	-	11.493
Gaussian	OT	PI	0.0049	1.1278	0.1277	0.1128	0.0128	29.221	1.2490	2.7250	19.787
		MPC	0.0109	1.1418	0.2323	0.1142	0.0232	7.8980	8.3440	16.232	18.365
		AMPC	0.0114	1.1348	0.2429	0.1135	0.0243	5.2610	6.8680	16.232	18.365
	DP	PI	0.0149	1.5157	0.3324	0.1516	0.0332	74.561	1.3400	4.8580	24.052
		MPC	0.0107	1.1342	0.2246	0.1134	0.0227	6.7300	8.3540	16.232	18.839
		AMPC	0.0086	1.0350	0.1739	0.1035	0.0174	2.3810	4.9710	10.308	14.810
Rayleigh	OT	PI	0.0050	0.7200	0.0830	0.0720	0.0083	29.221	1.1740	3.1990	17.891
		MPC	0.0092	1.1418	0.2323	0.1142	0.0232	6.1810	7.1870	15.995	17.654
		AMPC	0.0096	0.7808	0.1982	0.0781	0.0198	5.3960	6.4950	15.995	17.654
	DP	PI	0.0117	1.0262	0.2497	0.1026	0.0250	65.883	1.5280	4.8580	24.526
		MPC	0.0090	0.7960	0.1884	0.0796	0.0188	6.1590	7.0200	15.995	18.602
		AMPC	0.0070	0.6824	0.1336	0.0682	0.0134	5.6130	4.0600	15.995	17.910
Rician	OT	PI	0.0050	0.6594	0.0784	0.0659	0.0078	29.221	1.1600	2.7250	20.972
		MPC	0.0092	0.7535	0.1800	0.7530	0.0180	4.1300	7.8770	15.758	18.128
		AMPC	0.0096	0.7808	0.1982	0.0781	0.0198	2.9460	6.9890	15.758	18.126
	DP	PI	0.0048	0.8950	0.2300	0.0895	0.0230	65.833	1.5230	4.3840	21.209
		MPC	0.0088	0.7398	0.1746	0.0740	0.0175	4.1590	7.0160	16.469	18.605
		AMPC	0.0092	0.7348	0.1899	0.0735	0.0190	6.2690	3.9830	16.469	17.920
Uniform	OT	PI	0.0056	0.9314	0.0998	0.0931	0.0100	25.949	1.2450	2.4880	19.076
		MPC	0.0095	0.9828	0.1967	0.983	0.0197	4.8730	8.1630	16.706	18.602
		AMPC	0.0099	0.9768	0.2082	0.0977	0.0208	4.6550	6.4180	16.706	18.602
	DP	PI	0.0130	1.2885	0.2855	0.1288	0.0285	65.833	1.4290	4.6210	25.948
		MPC	0.0093	0.9736	0.1916	0.0974	0.0192	4.4810	7.6690	16.706	20.024
		AMPC	0.0074	0.8788	0.1454	0.0879	0.0145	6.1550	3.6660	16.706	20.024

for the parametric variations with an unsettled response, oscillations, and more overshoots. The proposed DAMPC performance is better than the PI and MPC controllers with quick settling time and reference tracking. Fig. 14, Fig. 15, and Fig. 16 show the VRM process's responses concerning reference tracking and disturbance rejection using different controllers. PI controller exhibits output responses within the constraints with overshoots. When time progresses, the PI controller tracks the set-points and provides acceptable rise-time, peak-time, and settling-time values. MPC controller responses show that no overshoot and within the constraints. The proposed DAMPC controller responses show no overshoot present in both input and output variables with quick settling time. The proposed control's overall performance is suitable for reference tracking and disturbance rejection compared to other existing controllers. The complete results with error metrics and time response specification values are summarized in Table 7.

V. CONCLUSION

The correlation method is quite satisfactory for the selection of the process variables for MIMO systems. State-space models are preferable because of intermediate states availability and direct adaption in traditional, classical, and modern control methodologies. The accurate pairing of controlled and manipulated variables is a difficult task, even misleads for dynamic systems. The control methods like PID, Ratio logic, and Fuzzy logic originate the plant's untimely shut down because of poor disturbance rejection of slowly varying signals. Designing a PID controller is more complicated for multi-variable system; this can overcome using proposed data-based modeling and modern control methods. The MPC is well suited for reference tracking and disturbance rejection for multi-variable systems with off-line parameter estimation. The proposed DAMPC is accurate in handling the parametric variations present in the dynamic systems.

In the future, composite learning and concurrent learning methods may be used for VRM modeling and on-line parameter estimation to handle MIMO systems' dynamics. The tuning of DAMPC parameters may be performed using soft-computing methods (like a genetic algorithm, neural networks) to select the optimal prediction and control horizon values instead of manual tuning. Implementation of these methods takes more implementation and optimization problem-solving time, also sometimes leads to system instability.

REFERENCES

[1] M. J. Knoflicek and W. C. Wentzel, "Experiences with clinker grinding in roller mills," *IEEE Trans. Ind. Appl.*, vol. 31, no. 2, pp. 413–418, Apr. 1995.

[2] N. A. Toprak, A. H. Benzer, C. E. Karahan, and E. S. Zencirci, "Effects of grinding aid dosage on circuit performance and cement fineness," *Construct. Building Mater.*, vol. 265, pp. 120707–120715, Dec. 2020.

[3] N. A. Madlool, R. Saidur, M. S. Hossain, and N. Rahim, "A critical review on energy use and savings in the cement industries," *Renew. Sustain. Energy Rev.*, vol. 15, no. 4, pp. 2042–2060, 2011.

[4] A. Atmaca and N. Atmaca, "Determination of correlation between specific energy consumption and vibration of a raw mill in cement industry," *Anadolu Üniversitesi Bilim Ve Teknoloji Dergisi A-Uygulamalı Bilimler ve Mühendislik*, vol. 17, no. 1, pp. 209–219, 2016.

[5] L. I. Minchala, Y. Zhang, and L. Garza-Castañón, "Predictive control of a closed grinding circuit system in cement industry," *IEEE Trans. Ind. Electron.*, vol. 65, no. 5, pp. 4070–4079, May 2018.

[6] D. Altun, H. Benzer, N. Aydogan, and C. Gerold, "Operational parameters affecting the vertical roller mill performance," *Minerals Eng.*, vols. 103–104, pp. 67–71, Apr. 2017.

[7] O. Altun, H. Benzer, E. Karahan, S. Zencirci, and A. Toprak, "The impacts of dry stirred milling application on quality and production rate of the cement grinding circuits," *Minerals Eng.*, vol. 155, Aug. 2020, Art. no. 106478.

[8] T. Tamashige, H. Obana, and M. Hamaguchi, "Operational results of OK series roller mill," *IEEE Trans. Ind. Appl.*, vol. 27, no. 3, pp. 416–424, Jun. 1991.

[9] J. A. Swanepoel, C. J. Boshoff, and E. H. Mathews, "The cost effects of DSM interventions on vertical roller mills in the cement industry," in *Proc. Int. Conf. 11th Ind. Commercial Use Energy*, Aug. 2014, pp. 1–4.

[10] B. V. Bhaskar and S. Jayalalitha, "Process control for cement grinding in vertical roller mill (VRM) a review," *ARPN J. Eng. Appl. Sci.*, vol. 20, no. 20, pp. 5758–5765, 2006.

[11] M. Boulvin, A. V. Wouwer, R. Lepore, C. Renotte, and M. Remy, "Modeling and control of cement grinding processes," *IEEE Trans. Control Syst. Technol.*, vol. 11, no. 5, pp. 715–725, Sep. 2003.

[12] L. Zhang, Q. Zhang, and J. Liu, "Application of fractional order controller for vertical roller mill outlet temperature," in *Proc. Chin. Autom. Congr. (CAC)*, Dec. 2018, pp. 926–929.

[13] M. Simmons, L. Gorby, and J. Terembula, "Operational experience from the United States' first vertical roller mill for cement grinding," in *Proc. Conf. Rec. Cement Ind. Tech. Conf.*, May 2005, pp. 241–249.

[14] A. K. Pani and H. K. Mohanta, "Soft sensing of particle size in a grinding process: Application of support vector regression, fuzzy inference and adaptive neuro fuzzy inference techniques for online monitoring of cement fineness," *Powder Technol.*, vol. 264, pp. 484–497, Sep. 2014.

[15] M. Zhu, Y. Ji, Z. Zhang, and Y. Sun, "A data-driven decision-making framework for online control of vertical roller mill," *Comput. Ind. Eng.*, vol. 143, May 2020, Art. no. 106441.

[16] A. K. Pani and H. K. Mohanta, "Online monitoring and control of particle size in the grinding process using least square support vector regression and resilient back propagation neural network," *ISA Trans.*, vol. 56, pp. 206–221, May 2015.

[17] J. Zheng, W. Du, I. Nascu, Y. Zhu, and W. Zhong, "An interval type-2 fuzzy controller based on data-driven parameters extraction for cement calciner process," *IEEE Access*, vol. 8, pp. 61775–61789, 2020.

[18] J. Dombi and A. Hussain, "A new approach to fuzzy control using the distending function," *J. Process Control*, vol. 86, pp. 16–29, Feb. 2020.

[19] C. Woywadt, "Grinding process optimization—Featuring case studies and operating results of the modular vertical roller mill," in *Proc. IEEE-IAS/PCA Cement Ind. Tech. Conf.*, May 2017, pp. 1–7.

[20] S. J. Qin and T. A. Badgwell, "A survey of industrial model predictive control technology," *Control Eng. Pract.*, vol. 11, no. 7, pp. 733–764, 2003.

[21] E. Atam, "Investigation of the computational speed of Laguerre network-based MPC in the thermal control of energy-efficient buildings," *Turkish J. Electr. Eng. Comput. Sci.*, vol. 25, no. 5, pp. 4369–4380, 2017.

[22] E. Suwartadi, V. Kungurtsev, and J. Jäschke, "Fast sensitivity-based economic model predictive control for degenerate systems," *J. Process Control*, vol. 88, pp. 54–62, Apr. 2020.

[23] N. Yan-Yan, Z. Guang, Y. Ming-Zhe, and W. Zhuo, "Design of intelligent control system for vertical roller mill," in *Proc. 2nd Int. Conf. Intell. Control Inf. Process.*, vol. 1, Jul. 2011, pp. 315–318.

[24] Q. Meng, Y. Wang, F. Xu, and X. Shi, "Control strategy of cement mill based on bang-bang and fuzzy PID self-tuning," in *Proc. IEEE Int. Conf. Cyber Technol. Autom., Control, Intell. Syst. (CYBER)*, Jun. 2015, pp. 1977–1981.

[25] M. Authenrieth, T. Hyttrek, A. Reintke, and S. McGarel, "ILM-master for VRMs," *Int. Cement Rev.*, May 2012.

[26] J. D. Le Roux, L. E. Olivier, M. Naidoo, R. Padhi, and I. K. Craig, "Throughput and product quality control for a grinding mill circuit using non-linear MPC," *J. Process Control*, vol. 42, pp. 35–50, Jun. 2016.

[27] L. Magni, G. Bastin, and V. Wertz, "Multivariable nonlinear predictive control of cement mills," *IEEE Trans. Control Syst. Technol.*, vol. 7, no. 4, pp. 502–508, Jul. 1999.

[28] B. V. Bhaskar and S. Jayalalitha, "Comparison of various models implemented using linear and non-linear system identification methods for cement grinding process using a vertical roller mill," *Int. J. Mech. Prod. Eng. Res. Develop.*, vol. 8, no. 2, pp. 137–148, 2018.

[29] L. Ljung, "System identification," in *Wiley Encyclopedia of Electrical and Electronics Engineering*. Hoboken, NJ, USA: Wiley, 1999, pp. 1–19.

[30] A. Mohammed, C. Naugler, and B. H. Far, "Emerging business intelligence framework for a clinical laboratory through big data analytics," in *Emerging Trends in Computational Biology, Bioinformatics, and Systems Biology: Algorithms and Software Tools*. New York, NY, USA: Elsevier/Morgan Kaufmann, 2015, pp. 577–602, 2015.

[31] W. Belhaj and O. Boubaker, "MIMO PI controllers for LTI systems with multiple time delays based on ILMIs and sensitivity functions," *Math. Problems Eng.*, vol. 2017, Feb. 2017, Art. no. 1241545.

[32] Y. Gu and F. Ding, "Auxiliary model based least squares identification method for a state space model with a unit time-delay," *Appl. Math. Model.*, vol. 36, no. 12, pp. 5773–5779, 2012.

[33] S. Pang, Q. Li, and H. Zhang, "A new online modelling method for aircraft engine state space model," *Chin. J. Aeronaut.*, vol. 33, no. 6, pp. 1756–1773, 2020.

[34] B. L. Pence, H. K. Fathy, and J. L. Stein, "Recursive maximum likelihood parameter estimation for state space systems using polynomial chaos theory," *Automatica*, vol. 47, no. 11, pp. 2420–2424, 2011.

[35] W.-X. Zhao, W. X. Zheng, and E.-W. Bai, "A recursive local linear estimator for identification of nonlinear ARX systems," *IFAC Proc. Volumes*, vol. 45, no. 16, pp. 1517–1522, 2012.

[36] A. Fatehi and A. Shariati, "Automatic pairing of MIMO plants using normalized RGA," in *Proc. Medit. Conf. Control Autom.*, Jun. 2007, pp. 1–6.

[37] B. Boudjehem and D. Boudjehem, "Fractional PID controller design based on minimizing performance indices," *IFAC-PapersOnLine*, vol. 49, no. 9, pp. 164–168, 2016.

[38] A. Tepljakov, B. B. Alagoz, C. Yeroglu, E. Gonzalez, S. H. HosseinNia, and E. Petlenkov, "Fopid controllers and their industrial applications: A survey of recent results," *IFAC-PapersOnLine*, vol. 51, no. 4, pp. 25–30, 2018.

[39] H. Tuan, A. Savkin, T. Nguyen, and H. Nguyen, "Decentralised model predictive control with stability constraints and its application in process control," *J. Process Control*, vol. 26, pp. 73–89, Feb. 2015.

[40] M. Guay, V. Adetola, and D. DeHaan, *Robust and Adaptive Model Predictive Control of Nonlinear Systems*. London, U.K.: Institution Engineering Technology, 2015.

[41] D. W. Clarke, "Application of generalized predictive control to industrial processes," *IEEE Control Syst. Mag.*, vol. 8, no. 2, pp. 49–55, Apr. 1988.

[42] K. Kumar, T. A. N. Heirung, S. C. Patwardhan, and B. Foss, "Experimental evaluation of a MIMO adaptive dual MPC," *IFAC-PapersOnLine*, vol. 48, no. 8, pp. 545–550, 2015.

[43] V. Adetola and M. Guay, "Robust adaptive MPC for constrained uncertain nonlinear systems," *Int. J. Adapt. Control Signal Process.*, vol. 25, no. 2, pp. 155–167, 2011.

[44] S. Zhang, L. Dai, and Y. Xia, "Adaptive MPC for constrained systems with parameter uncertainty and additive disturbance," *IET Control Theory Appl.*, vol. 13, no. 15, pp. 2500–2506, 2019.

[45] T. Liu, L. Li, G. Shao, X. Wu, and M. Huang, "A novel policy gradient algorithm with PSO-based parameter exploration for continuous control," *Eng. Appl. Artif. Intell.*, vol. 90, Apr. 2020, Art. no. 103525.

[46] S. Jiang, S.-C. Fang, T. Nie, and W. Xing, "A gradient descent based algorithm for lp minimization," *Eur. J. Oper. Res.*, vol. 283, no. 1, pp. 47–56, 2020.

[47] T. A. N. Heirung, B. E. Ydstie, and B. Foss, "An MPC approach to dual control," *IFAC Proc. Volumes*, vol. 46, no. 32, pp. 69–74, 2013.

[48] A. O. Shuaib and M. M. Ahmed, "The effect of parameter variation on open and closed loop of control system sensitivity," *Int. J. Innov. Res. Sci., Eng. Technol.*, vol. 3, no. 9, pp. 16355–16358, 2014.
[49] T. A. N. Heirung, B. E. Ydstie, and B. Foss, "Dual adaptive model predictive control," *Automatica*, vol. 80, pp. 340–348, Jun. 2017.

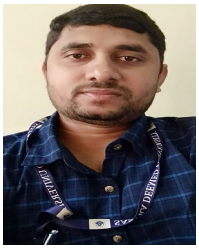

B. VIJAYABHASKAR was born in Andhra Pradesh, India. He received the B.Tech. degree in electronics instrumentation and control engineering and the M.E. degree in electronics and control engineering. He is currently pursuing the Ph.D. degree in cement grinding process control with SASTRA Deemed University.

He is also working as an Assistant Professor with the School of Electrical and Electronics Engineering, SASTRA Deemed University. His research interests include process control, modern control theory, instrumentation, embedded systems, cement grinding, and advanced control theory.

S. JAYALALITHA was born in Tamil Nadu, India. She received the B.E. degree in electronics and communication engineering, the M.E. degree in power systems, and the P.G.D.C.A. degree in computer applications, and the Ph.D. degree in instrumentation from the prestigious Indian Institute of Technology, Madras.

She is currently working as the Dean-Research of SASTRA Deemed University. Her primary research interests include distributed power generation, power engineering computing, R.L.C. circuits, active filters, building-integrated photovoltaics, compressors, control engineering computing, control system synthesis, crops, distribution networks, electric current control, field-programmable gate arrays, fuzzy logic, impedance matching, inductive power transmission, inductors, industrial plants, ladders, load (electric), load flow, motorcycles, operational amplifiers, passive networks, power grids, and harmonic power filters.